Random Forest and deep learning approaches for detecting forest cover changes

Oleh Chaskovskyy[1,†], Oleksiy Sinkevych[2,**,‡], Serhii Havryliuk[2,‡], Andriy Nechepurenko[2,‡], Oksana Pelyukh[2,‡] and Mykola Rozumovskyi[2,‡]

[1]*Institute of Ecology of the Carpathians of the National Academy of Science of Ukraine, 4 Kozelnytska Str., Lviv, 79026, Ukraine*
[2]*Ukrainian National Forestry University, 103 Henerala Chuprynky Str., Lviv, 79057, Ukraine*

Abstract

The forests of the Ukrainian Carpathians, particularly within the National Nature Park "Skole Beskids", face increasing pressures from climate change and anthropogenic activities. Disturbances ranging from extreme weather events to illegal logging undermine forest health and ecosystem stability. Timely, data-driven monitoring is therefore essential for sustainable forest management. This study applies a multi-sensor remote sensing approach to detect forest cover changes in the Skole Beskids between 2023 and 2024, combining Sentinel-1 synthetic aperture radar (SAR) data, Sentinel-2 multispectral imagery, and a Global Digital Elevation Model (DEM). Sentinel-2 provides detailed optical information on vegetation health and canopy cover, while Sentinel-1 enhances structural change detection under cloudy conditions and dense canopy. A comparison was conducted between a traditional machine learning method (Random Forest, RF) and a deep learning approach (UNet with a ResNet34 backbone) for robust classification and semantic segmentation. The deep learning model demonstrated superior performance in boundary delineation and noise reduction, achieving high accuracy on the validation dataset: an Intersection over Union (IoU) of 0.84, an F1-score of 0.91, a Pixel Accuracy of 0.96, an Overall Accuracy of 83.81%, and a Kappa coefficient of 0.676. Analysis of the 2023–2024 period identified approximately 1.247 square km of forest cover change within the park boundaries. The integration of multi-sensor data and AI-based analysis enabled accurate medium-resolution mapping and improved classification reliability. This research demonstrates the potential of an operational, multi-sensor satellite monitoring framework to support forest governance and conservation strategies in the Ukrainian Carpathians.

Keywords

remote sensing, machine learning, deep learning, artificial neural network, DEM, forest disturbances, SAR, multispectral imagery, decision support, Ukrainian Carpathians, human-computer interaction

1. Introduction

Forests of the Carpathian region are under persistent pressure from both climate change and anthropogenic activities [1]. While the impacts of climate change evolve gradually, they manifest through phenomena such as prolonged droughts, pest outbreaks [2], and shifts in species composition [3]. In contrast, human-induced disturbances, particularly clear-cutting, produce rapid and often compounding effects, amplifying the vulnerability of forest ecosystems to climate-related stressors [4].

In the Ukrainian Carpathians, illegal logging remains a significant challenge [5, 6], causing large-scale damage to forests and adjacent ecosystems. Consequences include soil erosion, altered hydrological regimes, and habitat fragmentation, often exacerbated by insufficient forest management practices. Traditional forest inventory and monitoring methods in Ukraine have notable limitations, hindering the timely detection of disturbances and allowing illegal activities to persist.

CS&SE@SW 2025: 8th Workshop for Young Scientists in Computer Science & Software Engineering, November 21, 2025, Kryvyi Rih, Ukraine
https://doi.org/10.55056/cssesw2025/paper22
**Corresponding author.
‡These authors contributed equally.
oleh.chaskov@nltu.edu.ua (O. Chaskovskyy); oleksiy1694@gmail.com (O. Sinkevych); serhiy_havrylyuk@nltu.edu.ua (S. Havryliuk); andriy.nechepurenko@gmail.com (A. Nechepurenko); pelyukh.o@nltu.edu.ua (O. Pelyukh); mykolarozumovskyy@nltu.edu.ua (M. Rozumovskyi)
0000-0002-2938-0524 (O. Chaskovskyy); 0000-0001-6651-5494 (O. Sinkevych); 0000-0003-0361-0624 (S. Havryliuk); 0000-0003-3955-1849 (A. Nechepurenko); 0000-0002-1889-3623 (O. Pelyukh); 0009-0003-7291-811X (M. Rozumovskyi)

The integration of satellite remote sensing into forest monitoring offers a cost-effective and scalable alternative for improving detection accuracy [7, 8]. In particular, the combined use of Sentinel-1 synthetic aperture radar (SAR) data, Sentinel-2 multispectral imagery, and Digital Elevation Models (DEM) provides complementary insights into forest conditions [9, 10]. Sentinel-2 offers high-resolution optical information on vegetation health and canopy cover, while Sentinel-1 SAR penetrates cloud cover and detects structural changes even in densely forested areas [11, 12, 13].

Beyond traditional classification techniques, the application of deep learning-based image segmentation enables more precise and reliable delineation of forest boundaries. Neural network architectures, such as UNet and ResNet-based convolutional models, can capture complex spatial patterns and contextual information in remote sensing imagery, improving the accuracy of forest disturbance mapping and reducing the influence of noise or mixed pixels [14].

The objective of this study is to develop and test a multi-sensor, satellite-based methodology for detecting forest cover changes in the Ukrainian Carpathians. By leveraging multi-temporal SAR and optical datasets, combined with advanced machine learning and deep learning methods, the proposed approach aims to deliver accurate, actionable results for forest protection, supporting both large-scale assessments and the investigation of specific forest loss events.

The scientific novelty of this study lies not in the isolated application of these methods, but in their integrated, end-to-end workflow tailored for operational monitoring in the Ukrainian Carpathians. Unlike previous studies that often focus either on RF or DL in isolation, we conduct a direct comparison within this specific ecosystem. Crucially, we develop and demonstrate a complete pipeline from multi-sensor data processing (Sentinel-1 SAR, Sentinel-2 Optical, and DEM) in Google Earth Engine to the automated deployment of UNet segmentation results via a custom API to an interactive Web GIS platform, thus bridging the gap between remote sensing analysis and on-the-ground decision-making [15].

2. Study area and dataset

2.1. Area of interest

Ukraine is characterized by diverse natural conditions, ranging from the mixed forest zone in the north to forest-steppe and steppe landscapes in the south. Two mountainous regions are present the Ukrainian Carpathians and the Crimean Mountains each with distinctive forest cover characteristics. In the north, forests occupy vast areas, while in the steppe zone they are primarily represented by shelterbelts and small forest patches. The Ukrainian Carpathians are predominantly forested, with a current forest cover of 42%, compared to an estimated optimal value of approximately 45% [16].

The National Nature Park "Skole Beskids" (NNP Skole Beskids) was established in 1999, encompassing an area of 35,684 ha in the Lviv administrative region (figure 1). It is located in the southern part of the Lviv region and the northern part of the Ukrainian Carpathians. The park's forests are dominated by beech (Fagus sylvatica) and fir (Abies alba) stands, with smaller occurrences of spruce (Picea abies) and black alder (Alnus glutinosa). Mixed stands include sycamore maple (Acer pseudoplatanus), Norway maple (Acer platanoides), rock elm (Ulmus glabra), common hornbeam (Carpinus betulus), and common ash (Fraxinus excelsior) [17].

The NNP Skole Beskids is a protected area divided into four functional zones:

- Core zone – 23.4% of the territory, under the strictest protection;
- Regular recreation zone – 35.3%;
- Stationary recreation zone – 0.4%;
- Management zone – 40.9%, where regulated economic activity is permitted.

Forests surrounding the park are managed by forestry enterprises, which may influence the park's integrity due to potential intrusions into its protected boundaries. Geomorphologically, the NNP lies within the middle-mountain zone, with elevations reaching up to 1,200 m above sea level [18]. Forests

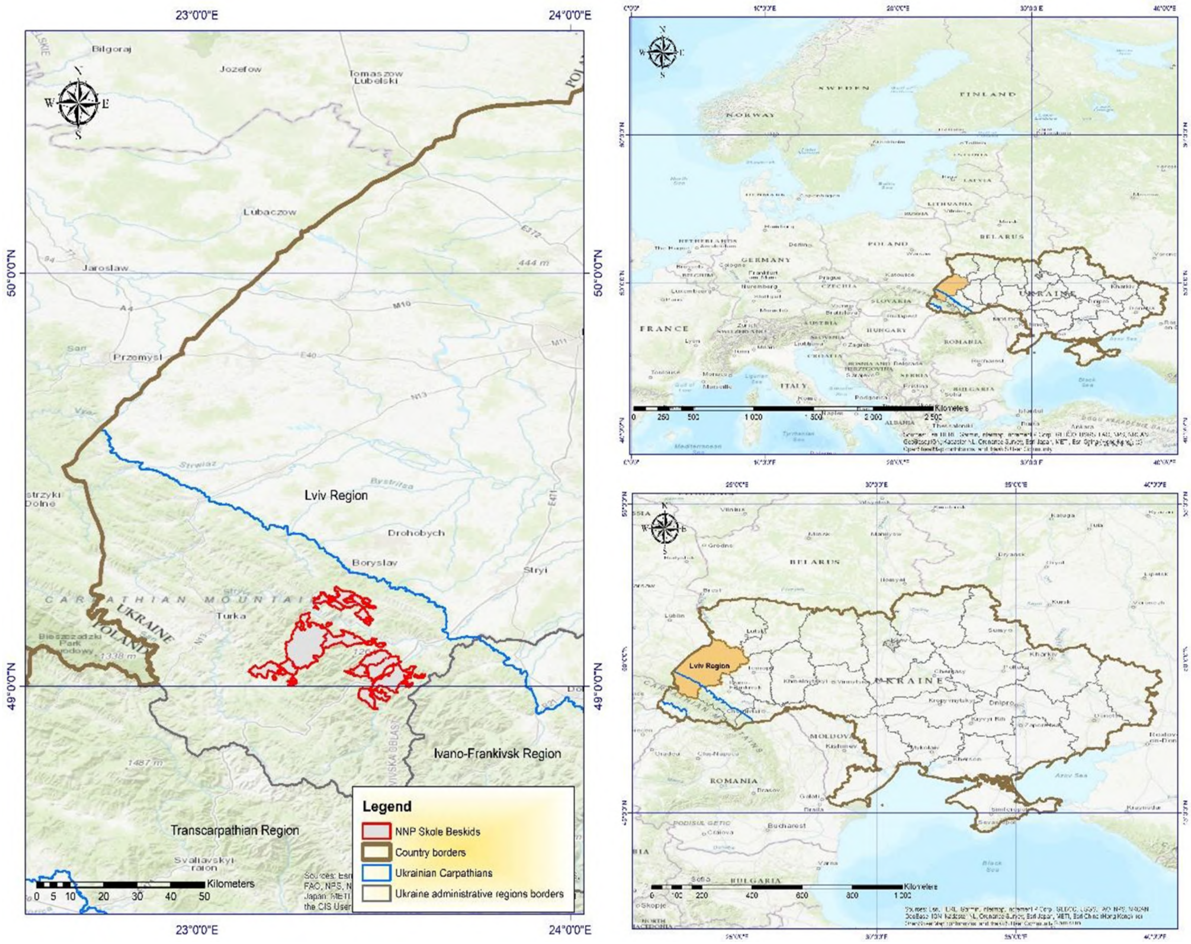

Figure 1: Area of interest: (top right) Ukraine on a map of Europe; (bottom right) administrative divisions of Ukraine; (left) territory of the NNP Skole Beskids

cover approximately 88.4% of the park's territory, of which about 40% are artificial plantations [18]. The area harbors a rich diversity of flora and fauna, including numerous protected species. Notably, in the 1970s, the European bison (Bison bonasus) was reintroduced into the park.

2.2. Satellite images

Satellite imagery provides a robust basis for analysing forest disturbances, offering data at multiple spatial resolutions and temporal frequencies. In this study, freely available Sentinel-2 Surface Reflectance (Level-2A) imagery was accessed via the Google Earth Engine platform. These datasets, provided by the European Space Agency's Copernicus Programme, are available from 28 March 2017 to the present, fully covering the study period.

Sentinel-2 data include 12 primary spectral bands with spatial resolutions of 10 m, 20 m, and 60 m, as well as 11 additional synthetic bands generated for specialised applications such as cloud and snow masking. Since February 2024, three bitmask layers have also been available, allowing the identification of opaque clouds, cirrus clouds, and snow/ice. In this study, synthetic bands were primarily used to mask clouds and their shadows.

Additionally, synthetic vegetation index bands were employed. While the Normalized Difference Vegetation Index (NDVI) remains one of the most widely used indices for assessing vegetation health [19], other indices can provide complementary insights. In particular, the Enhanced Vegetation Index (EVI) was selected in this study, as it offers improved sensitivity to high-biomass regions and better performance in areas with dense canopy cover.

Given the mountainous terrain of the study area - with variations in elevation, slope steepness, and illumination conditions – topographic correction was supported by Shuttle Radar Topography Mission (SRTM) digital elevation data [20]. These data help mitigate the effects of terrain-induced reflectance variability, improving the interpretability of optical imagery in complex landscapes.

The training and validation datasets were derived using land cover information from the Copernicus Global Land Service (CGLS) program [21]. The CGLS dataset provides a global land cover map for 2019 with a spatial resolution of 100 m. Random sampling points were generated within the boundary envelope of the NNP Skole Beskids, and the corresponding land cover class was assigned to each point.

The CGLS classification scheme includes 23 land cover classes, of which several correspond to forest vegetation. Six classes describe closed tree stands:

- Closed forest, evergreen needle leaf;
- Closed forest, evergreen broad leaf;
- Closed forest, deciduous needle leaf;
- Closed forest, deciduous broad leaf;
- Closed forest, mixed;
- Closed forest, not matching any of the other definitions.

For the purposes of this study, all six closed forest classes were merged into a single "forest" category. In addition, open forest classes (e.g., Open Forest, evergreen needle leaf, where the canopy consists of 15–70% trees over a mixed shrub and grassland layer, with predominantly needle leaf species retaining green foliage year-round) were also incorporated into the "forest" category. All other CGLS classes were assigned to the "non-forest" category.

From the resulting dataset, 700 randomly selected forest and non-forest points were used for model training. An additional 300 randomly selected points per class were reserved for independent validation (figure 2). Some of the sampled points were cross-verified using auxiliary datasets, including forest management maps of the NNP Skole Beskids and high-resolution satellite imagery available in Google Earth.

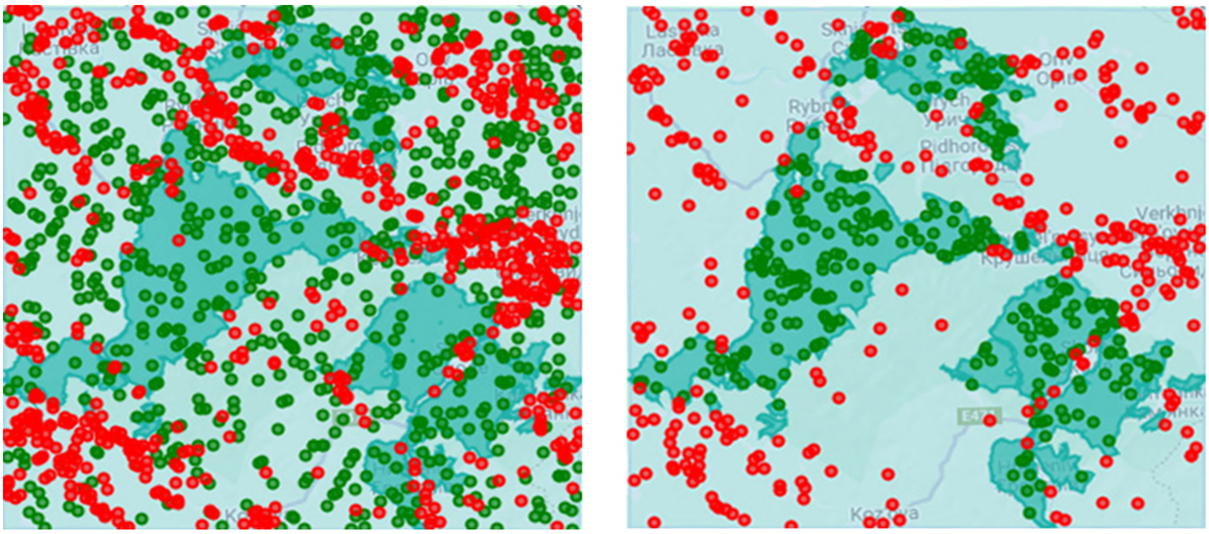

Figure 2: Training and checking points for the classification (left – training points; right – checking points). Light blue – envelope; dark green – boundaries of NNP Skole Beskids; green dots – forest; red dots – non-forest.

3. Methodology

3.1. Preprocessing and remote sensing data handling

Sentinel-2 Surface Reflectance (Level-2A) data include both optical spectral bands and synthetic bands designed for specific processing tasks, such as masking cloud cover, cloud shadows, snow, and ice. In this study, only the vegetation period (June-September) was analyzed, thereby excluding snow and ice from consideration.

Cloud and shadow masking was performed in Google Earth Engine (GEE) using a custom script [22, 23, 24]. Two Sentinel-2 quality layers were employed:

- MSK_CLDPRB (Cloud Probability Mask) – pixels with cloud probability >50% were masked;
- SCL (Scene Classification Layer) – classes Clouds Medium Probability, Clouds High Probability, and Cirrus were masked.

Masked pixels were assigned a value of 0 and excluded from subsequent classification. If a training or validation point intersected a masked pixel for a given acquisition date, the corresponding observation was omitted from model training and validation.

For deep learning processing, median composites were generated in GEE for Sentinel-2 tile 34UFV, which fully encompasses the study area. A dedicated script applied the aforementioned cloud and shadow filtering to all imagery prior to compositing. To explore optimal input configurations for forest cover change detection, multiple composite types were produced for 2023 and 2024 using imagery from June 1 to September 30:

- RGB composite – bands B4 (red), B3 (green), B2 (blue).
- CIR composite – bands B8 (near-infrared), B4 (red), B3 (green).
- Four-band 10 m composite – bands B2, B3, B4, B8.
- Two-year median composite – all 10 m bands, generated for 2022-2023 and 2023-2024 separately.
- Topography-enhanced composite – all 10 m bands + SRTM-derived elevation and slope layers.
- Multi-sensor composite – all 10 m bands + SRTM (elevation, slope) + Sentinel-1 SAR VV and VH polarizations.

Each composite type was evaluated separately during the deep learning stage to assess its contribution to classification performance.

3.2. Random forest classification

The Random Forest (RF) classifier is one of the most widely used supervised classification algorithms for remote sensing image interpretation. RF is an ensemble method based on multiple decision trees, offering high classification accuracy while reducing the risk of overfitting [25, 26]. It has been successfully applied in various domains, including land cover mapping [27], forest monitoring [28, 29], and even astronomical studies [30]. Key advantages of the Random Forest algorithm include [25, 31]:

- Classification accuracy comparable to, and in some cases exceeding, that of AdaBoost.
- Robustness to outliers and noise.
- Faster execution compared to bagging or boosting methods.
- The ability to provide internal estimates of error rates, classifier strength, correlation, and variable importance.
- A relatively simple structure that is easily parallelized.

Due to these advantages, RF is implemented in multiple programming environments, including JavaScript. In this study, RF classification was conducted in Google Earth Engine (GEE) using the ee.Classifier.smileRandomForest() operator, configured with 50 decision trees.

For the Random Forest classification in Google Earth Engine (GEE), all possible bands from the Sentinel-2 Surface Reflectance images for the years 2023 and 2024 were used. In particular, there were included all optical bands and additionally, AOT (Aerosol Optical Thickness), WVP (Water Vapor Pressure), and SCL (Scene Classification Map). For the clouds and shadows masking the SCL band, the special 'MSK_CLDPRB' (Cloud Probability Map) band was used. All these bands were included for the classification with the Random Forest Algorithm in GEE.

The accuracy of classification using the Random Forest algorithm was assessed using the most commonly used coefficients in practice, namely Overall Accuracy and Kappa coefficient. Overall accuracy consists of evaluating correctly classified pixels from the validation data set in the confusion matrix. Overall accuracy is calculated using the formula:

$$P_{overall} = \frac{\sum_{i=1}^{k} n_{ij}}{N} \times 100 \tag{1}$$

where n_{ij} – the number of pixels, which were correctly classified to class i; N – total amount of pixels; k – amount of classes, included into the classification.

The kappa coefficient is the de facto standard for evaluating agreement between raters, which factors out expected agreement due to chance. This coefficient is calculated based on the confusion matrix and is calculated using the formula:

$$K = \frac{N \sum_{i=1}^{r} x_{ii} - \sum_{i=1}^{r} (x_{i+} * x_{+i})}{N^2 - \sum_{i=1}^{r} (x_{i+} * x_{+i})} \tag{2}$$

where r – the number of rows in confusion matrix, x_{ii} – number in row i and column i; x_{i+} - the sum for row i; x_{+i} – the sum of column i.

The accuracy of the classification using Random Forest algorithm was made using these two statistics.

3.3. Neural network implementation

To train the neural network, the PyTorch library is used. This extension is created in Python and allows you to build, train and run neural networks with high performance [32], especially on GPUs. In the code, the use of the library is displayed by the following fragment:

```
import segmentation\_models as sm
import segmentation\_models\_pytorch as smp
import segmentation\_models\_pytorch.utils
import torch from torch.utils.data
import DataLoader
import tensorflow as tf
```

Justification for the use of this library, it is enough to highlight the main characteristics, which are:

- Dynamic computational graphs: models are created quickly enough, which simplifies debugging and experimentation.
- Automatic gradient calculation: the autograd module makes it easy to implement backpropagation errors.
- GPU Support: Computations can be significantly accelerated through CUDA.
- Intuitive syntax: reminiscent of NumPy, but with the ability to work with tensors on the GPU.
- Flexibility for research and production: suitable for both prototyping and scalable solutions.

To get a detailed understanding of the algorithm, you need to go through the stages of creating a neural network in PyTorch and integrate it with the GPU. So, in the first step, you need to import the settings.see above. Next, the GPU is configured. In it, you need to select the device on which the result will be processed. In the program code, this is reflected in the following snippet:

```
        DEVICE = torch.device("cuda" if torch.cuda.is_available() else "cpu")
```

At the second stage, the model is defined. In our case, there is a breakdown Four-channel Images in small fragments with an extension 64x64. After that, we move on to the third stage, which is data uploading. It is displayed in the next two fragments. Namely, the selection of settings and the direct creation of a downloader of learning data from the class DataLoader pytorch based on SegmentationDataset:

```
        train_epoch = smp.utils.train.TrainEpoch(
                model,
                ...
                        device=DEVICE,
                verbose=True ,)
train_loader = DataLoader(gen, batch_size=64, shuffle=True, num_workers=0)
```

Once the data is loaded, we proceed to initialize the model and transfer to the GPU. The end of the work will be the training of the model and the preservation of the results. The following are code snippets:

```
model = SimpleModel().to(DEVICE)
max_rating = 0
for i in range(0, 20):
    train = train_epoch.run(train_loader)
    valid = valid_epoch.run(valid_loader)
    if max_rating < valid['iou_score']:
        max_rating = valid['iou_score']
        torch.save(model, 'save_model.pth')
```

Also separately should be noted the use of the cuBLAS library. It plays an important role in our algorithm and the PyTorch ecosystem. Among the specifications, it should be noted:

- Matrix multiplications (GEMM);
- Vector operations;
- Support mixed accuracy (FP16, TF32);
- Using Tensor Cores on Modern GPUs.

In PyTorch, cuBLAS is used automatically. Namely, PyTorch automatically calls cuBLAS to optimize computational processes, especially when working with CUDA tensors.

To summarize, let's make a resulting diagram (figure 3) of the operation of the software and describe the specification of each item.

Figure 3: Diagram of the algorithm.

1. *Preparing the environment.* At the initial stage, the environment for model training was set up. Google Drive was connected to enable saving and reading data directly from cloud storage. Next, the required libraries were installed, including egmentation_models_pytorch, rasterio, and other tools for working with satellite imagery and geospatial data. Modules from TensorFlow, PyTorch, OpenCV, scikit-learn, GDAL, and other libraries were imported to be used in data processing, preparation, and analysis stages.
2. *Data organization.* Once the environment was prepared, the input data were organized. Three separate directories were created: train_data containing sliced satellite image fragments, label_data_tr containing training masks, and label_data_val containing validation masks. The input images were multispectral (for example, eight channels) and had a fixed size of 64×64 pixels. The masks were single-channel and stored the classes used for segmentation tasks.

3. *Data Generator.* A custom SegmentationDataset class was used for loading the data. This class read images and their corresponding masks from disk, performed preprocessing that included image normalization and OneHot encoding of the masks, and generated batches for model training. It also supported data augmentation operations such as rotation and flipping, which improved the model's robustness.
4. *Building a segmentation model.* For semantic segmentation, the UNet architecture with a ResNet34 encoder was used. The model was configured to accept the required number of input channels (for example, four) and output classes (for example, two). The CrossEntropyLoss function was chosen as the loss function, while the Intersection over Union (IoU) metric was used to evaluate performance. The Adam optimizer was applied with a controlled learning rate for effective weight adjustment.
5. *Training cycle and visualization of results.* The training process consisted of the TrainEpoch and ValidEpoch stages. During training, the best-performing model achieving the highest IoU score was saved. The learning rate was adjusted in the fifth and fifteenth epochs. To analyze the segmentation quality and verify the correctness of the input data, masks were visualized using the Matplotlib library.
6. *Large Image Segmentation.* When working with large satellite images, they were divided into smaller tiles of 64×64 pixels. The model.predict function was applied to each tile, and the results were combined into a single array. Finally, the processed segmentation map was saved as a GeoTIFF file using the GDAL library.

3.4. Integration with Web GIS platform

The study area is located in the Skole Beskids region of the Ukrainian Carpathians, in the southern part of Lviv Oblast, covering an area of 57,966 hectares. The core of this region is the NNP Skole Beskids, which contains traditional nature park zones but also includes subcompartments managed by different authorities. Within the boundaries of the national park, there is a military-owned forest district where forest management activities are carried out intensively. This compact territory is of particular interest not only from an ecological perspective but also for studying the combined impact of natural and anthropogenic processes on forest ecosystems. The effects of these processes can be assessed using temporal remote sensing data.

Satellite imagery offers a valuable basis for detecting forest disturbances, as it is available at multiple spatial resolutions and time intervals. In this study, Sentinel-2 Surface Reflectance data (Level-2A), freely accessible via Google Earth Engine and provided through the European Space Agency's Copernicus Program, were used. The available dataset, covering the period from 28 March 2017 to the present, encompasses the entire study period. Sentinel-2 imagery includes 12 primary spectral bands with spatial resolutions ranging from 10 to 60 meters, as well as 11 additional synthetic bands used for specialized applications such as cloud and snow masking. Since February 2024, three bitmask layers have also been available to identify opaque clouds, cirrus clouds, and snow/ice. In this research, the synthetic bands were primarily used for cloud and shadow masking.

The methodological approach is based on the assumption that different forest disturbance agents leave distinct spectral, spatial, and temporal footprints on satellite images before and after the disturbance event. Common disturbance agents include storm damage, insect infestations, drought-related dieback, and timber harvesting [33]. In this study, the focus was on detecting the extent of forest damage without differentiating between disturbance agents, as this would require additional data that could be incorporated in future investigations.

Deep learning methods are particularly well-suited for identifying patterns in spectro-temporal data series. The approach used here relies on the analysis of Sentinel-2 multispectral imagery from 2023–2024, providing high spatial and temporal resolution, within the Google Earth Engine environment. While traditional time-series tools in forest remote sensing tend to analyze the temporal spectral development of individual pixels or segments, such methods often overlook contextual spatial information.

Deep learning algorithms, such as convolutional neural networks, can integrate this additional context, making them increasingly important for image classification, land use monitoring, and incorporating auxiliary information (e.g., disturbance agent data from forestry enterprises). The combination of remote sensing and AI-based approaches remains a promising area for innovation in forest mapping, monitoring, and risk prediction systems. Previous work in related regions, such as the Prykarpattya area of Ukraine, has employed Random Forest classification for land cover analysis.

After processing the data in Google Earth Engine with Python, the trained algorithm was synchronized with a web-based GIS platform. The system was primarily designed to collect and display information on forest cover changes. A dedicated GIS web page was hosted using the Laravel framework and OctoberCMS. Data exchange between the Google Earth Engine–Python workflow and the web application was implemented via an API, which transmitted detected forest cover changes as data arrays.

The general structure of this workflow is shown in figure 4.

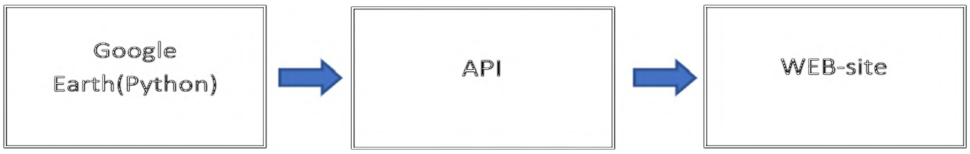

Figure 4: Synchronization.

The implemented Python function accepts a satellite image of the area of interest, processes it through a pre-trained neural network model, and records the detected changes into an array. This array is then written into a GeoTIFF raster file using GDAL and subsequently sent via an API request to the web application for storage and further analysis. The following code snippet illustrates this process:

```
    def get_tif(path, donkey):
model_path = 'save\_model.pth'
modelSave = torch.load(model_path, weights_only=False)
modelSave.eval()
output = gdal.Open('output.tif', 1)
input_map = rasterio.open(path)
image = input_map.read()
image = image / 1000
result = np.zeros((image.shape[1], image.shape[2]))
for i in range(0, image.shape[1] - 2*ker, 2*ker):
    for j in range(0, image.shape[2] - 2*ker, 2*ker):
        part = torch.from_numpy(np.array(image[:, i:i+2*ker, j:j+2*ker],dtype=np.float32))
        part = part.unsqueeze(0)
        predict= model.predict(part).squeeze().numpy().round().argmax(axis=0)
        result[i:i+2*ker, j:j+2*ker] = predict
        output.GetRasterBand(1).WriteArray(result)
        output = None
requests.post('http://site-test/setData', data=[output, result])
```

In this workflow, the processed satellite image is divided into smaller tiles, each of which is classified by the model. The results are aggregated into a single raster dataset and transmitted to the GIS platform for visualization and subsequent analysis.

4. Results

4.1. RF classification results

As mentioned above, to identify forested and non-forested areas within the “envelope” containing the boundaries of the NNP Skole Beskids, classification was performed using the RF algorithm. A training data set of 700 points of areas covered and not covered by forest vegetation was used, and 300 points of both classes were used to verify the accuracy of the classification. As an example, figure 5 shows the results of the classification with a distribution of areas covered and not covered by forest vegetation.

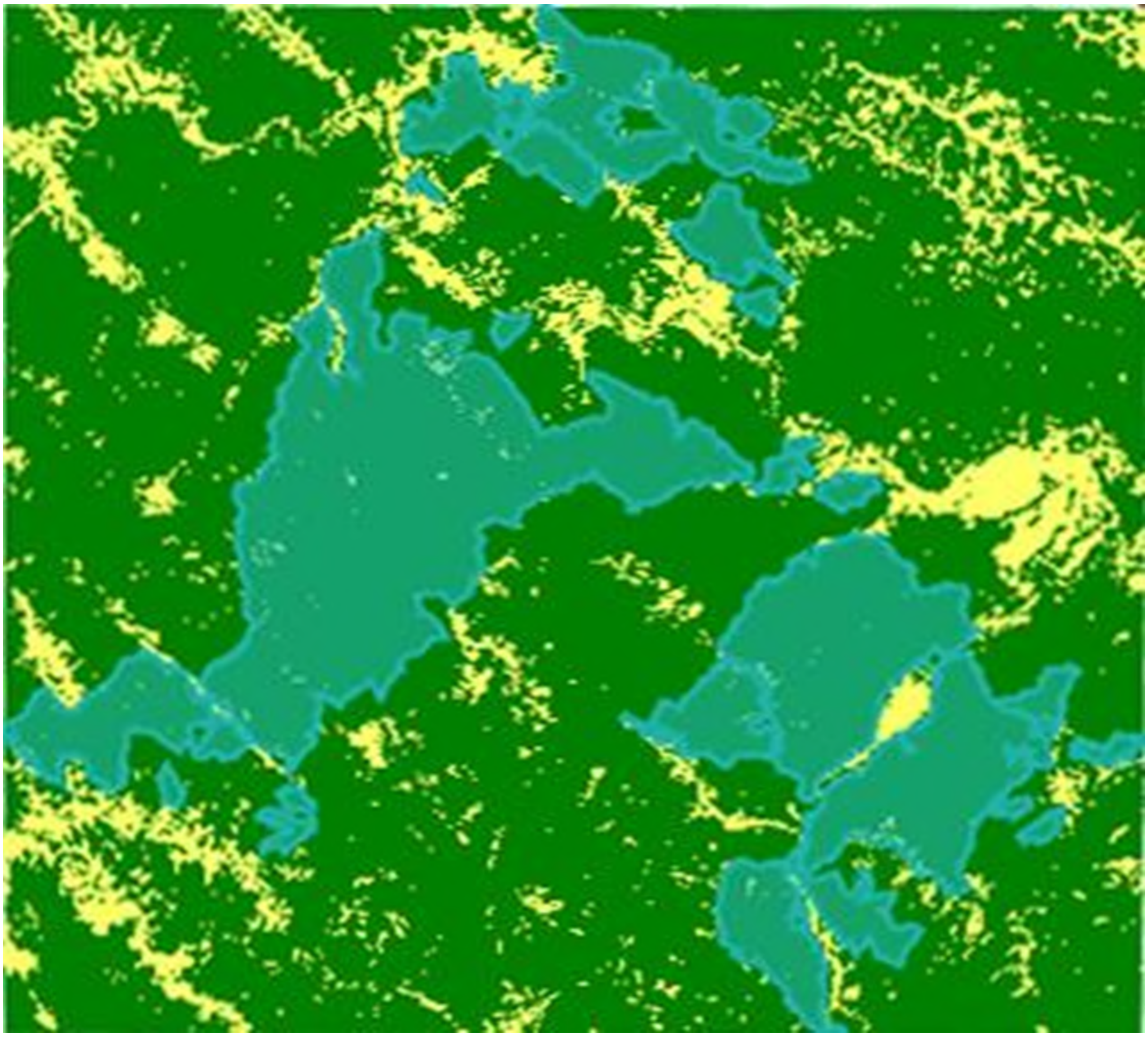

Figure 5: Classified image for the forest cover lands and non-forest cover lands.

Based on the results of the classification using images from 2023 and 2024, the accuracy of the classification was assessed. Table 1 shows the error matrix based on the classification results.

Table 1
The confusion matrix of the classification, ha.

Class	Forest	Non-forest	Total
Forest	296	4	300
Non-forest	93	207	300
Total	389	211	600

Based on the results of the classification accuracy check in the error matrix, the overall accuracy and kappa coefficient were calculated. Thus, the overall accuracy of the classification is 83.81%, while the kappa coefficient is only 0.676. Although these values indicate a satisfactory level of performance, they also highlight the potential for further improvement. Increasing classification accuracy would require expanding the size and diversity of the training and validation datasets, as well as integrating ground-truth data obtained through field surveys.

Following classification and accuracy assessment [34, 35, 36], changes in forest cover between 2023 and 2024 within the NNP Skole Beskids were quantified. This was accomplished by comparing the classified maps from both years and identifying areas where forest cover in 2023 had been converted to non-forest cover in 2024. The results of this change detection analysis are presented in figure 6.

Figure 6: Detection of the forest cover changes from 2023 to 2024 (red – detected changes).

As illustrated in figure 6, the majority of forest loss during the study period occurred outside the boundaries of the NNP Skole Beskids. To quantify these changes within the park, a zonal statistics algorithm was applied. The total forest change detected within the broader envelope area amounted to 8.176 square km, while within the park boundaries, deforestation was recorded over an area of 1.247 square km.

A more detailed investigation, conducted in collaboration with park staff, indicated that these changes were predominantly driven by biotic factors, namely spruce stand dieback and windthrow events occurring during the study period.

It should be noted that no filters were applied to the obtained data on forest cover changes, since it was assumed that even in a relatively small area, represented by 1 pixel measuring 10 by 10 m in the image, such changes could occur, mainly due to biotic factors. Since we are studying the territory of a national park where human intervention is minimal, the natural death of individual old-growth trees frees up space for the restoration of forest cover by the younger generation. Therefore, changes within the NNP Skole Beskids at a level of more than 1 km2 or 100 ha are the total area of all pixels identified as changes in forest cover.

4.2. Neural network results

The segmentation of the study area using the developed deep learning model provided high-quality binary classification of forest and non-forest areas. The analysis was carried out on Sentinel-2 multispectral imagery, preprocessed and normalized before being fed into the neural network. The evaluation focused both on visual inspection and on quantitative performance metrics, ensuring a comprehensive assessment of the model's accuracy and applicability for forest disturbance mapping. The main output example is presented in figure 7.

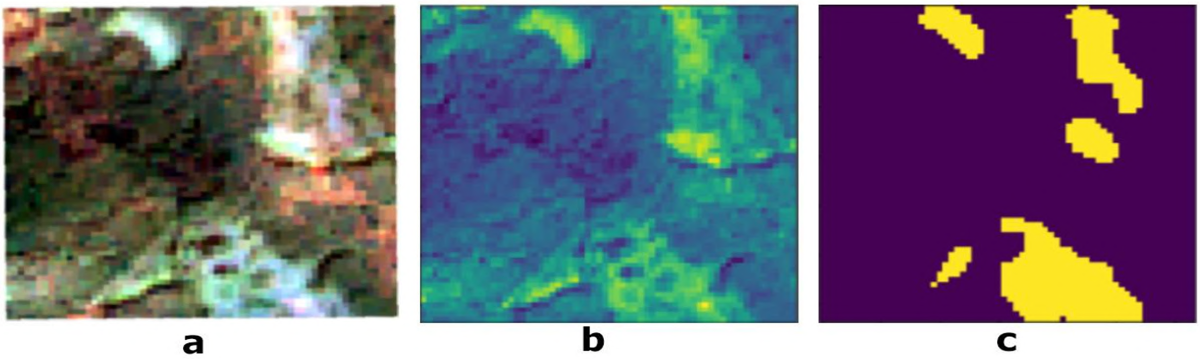

Figure 7: Segmentation results: a – original optical image of the study area; b – auxiliary single-channel spectral band representation; c – resulting binary segmentation mask.

Panel "a" shows the original optical image, which contains heterogeneous land cover types with varying textures and spectral signatures. This diversity makes automated classification challenging, particularly when certain non-forest elements share similar spectral characteristics with forest cover.

Panel "b" illustrates an auxiliary single-channel image (color gradient from blue to yellow) derived from one spectral band. Such intermediate representations are valuable for visualizing the spatial distribution of reflectance values, highlighting subtle boundaries and patterns that are not always visible in the true-color composite.

Panel "c" presents the final binary segmentation mask. Yellow areas correspond to the target class (e.g., forest disturbance zones), while purple represents the background. The model demonstrates strong capability in outlining objects with clear boundaries that align well with visible features in both the optical and spectral representations.

The quantitative evaluation on the validation dataset produced the following performance metrics:

- Intersection over Union (IoU): 0.84.
- F1-score (Dice coefficient): 0.91.
- Pixel Accuracy: 0.96.

These metrics confirm a high spatial agreement between the predicted masks and the reference data. The IoU of 0.84 reflects a substantial overlap with ground truth, while the F1-score indicates a balance between precision and recall. Pixel accuracy further verifies that the majority of pixels were classified correctly.

Despite the strong performance, minor misclassifications occurred in areas with high spectral similarity between forest and certain non-forest surfaces, such as early-stage agricultural fields or shadowed h[]

Table 2
Model performance comparison.

	Random Forest	Deep learning (UNet + ResNet34)
Overall Accuracy	83.81%	96.0% (Pixel Accuracy)
Kappa coefficient	0.676	N/A
Intersection over Union (IoU)	N/A	0.84
F1-score (Dice Coefficient)	N/A	0.91

slopes. Integrating additional vegetation indices (e.g., NDVI, NBR) and temporal imagery from multiple dates may improve class separability. Post-processing techniques, such as morphological filtering, could also help refine the segmentation boundaries.

From a forestry monitoring perspective, the segmentation results provide a robust foundation for detecting and mapping forest disturbances. The combination of visual consistency and high metric values makes this model suitable for integration into operational Web GIS systems for continuous forest monitoring.

4.3. Comparative analysis and computational efficiency

The comparative metrics in table 2 clearly demonstrate the superior segmentation performance of the UNet-based deep learning model over the traditional Random Forest classifier for this task. The UNet model's high IoU (0.84) and F1-score (0.91) indicate a much stronger capability for precise boundary delineation of forest disturbances, which was a key objective. The RF model, while satisfactory (83.81% accuracy), struggled more with the "salt-and-pepper" effect and mixed pixels, as evidenced by the lower Kappa coefficient (0.676).

The training and inference processes were evaluated to determine the system's operational viability. The model was trained in the Google Colab environment using a Tesla T4 GPU (16 GB VRAM). The environment also utilized 2 CPU cores and 12 GB of RAM.

The average training time per epoch was approximately 2–3 minutes with a batch size of 8 and an image size of 64×64 pixels. Full model training over 20 epochs took about 40–50 minutes.

Computational resources were used efficiently due to the optimized U-Net architecture with a ResNet34 encoder, which has approximately 21.3 million parameters. The GPU's video memory was sufficient to process batches of 8 images without exceeding the VRAM limit.

Although the deep learning model carries a higher computational cost for training, its significantly higher accuracy and reliability in segmentation justify its use for developing an operational monitoring system.

Time Complexity: O(N×H×W×C), where N is the number of images, H×W is the frame size, and C is the number of channels. Space Complexity: Proportional to the number of network parameters (≈ 85 MB when saved in .pth format). Inference for a single image (64×64 pixels) requires approximately 0.03 seconds on a GPU, or 0.4 seconds on a CPU. Thus, the model demonstrates high performance with moderate computational costs, allowing it to be used for batch processing of satellite imagery or for real-time tasks at resolutions up to 128×128 pixels.

5. Discussion and conclusion

This study demonstrated the effectiveness of combining freely available Sentinel-2 multispectral imagery, processed in Google Earth Engine, with deep learning-based segmentation methods for detecting forest disturbances in the NNP Skole Beskids [37]. The integration of auxiliary datasets, such as SRTM elevation data and vegetation indices (NDVI, EVI), allowed for improved interpretation of mountainous terrain and minimization of misclassifications in shadowed or spectrally complex areas.

The proposed segmentation model achieved high accuracy on the validation dataset (IoU = 0.84, F1-score = 0.91, Pixel Accuracy = 0.96), confirming its ability to reliably differentiate disturbed forest areas from intact forest cover. Analysis revealed a total forest loss of approximately 1.247 km2 during the 2023-2024 monitoring period, with the most affected zones located near commercial logging areas and within military forest districts. These findings are in line with previous research highlighting the combined impacts of human activities and climate variability on Carpathian forest ecosystems.

A key strength of the approach is its operational integration with a Web GIS platform, enabling automated transfer of processed data from Google Earth Engine to an online interface via API. This allows forest managers to visualize, analyze, and respond to disturbance events in near real time, making it possible to detect illegal logging earlier and assess the spatial extent of damage without relying solely on delayed field inspections.

Compared to traditional monitoring methods, the presented workflow is scalable, cost-efficient, and repeatable, providing consistent data across space and time. Such a framework contributes directly to the development of a Ukrainian National Forest Monitoring System, aligned with international standards. Incorporating additional datasets such as high-resolution radar or hyperspectral imagery, LiDAR data, meteorological records, and in-situ ground truth would further improve classification robustness and enable detection of specific disturbance agents.

Future research should explore multi-temporal analysis over longer periods, seasonal monitoring, and predictive modelling of disturbance risk. Scaling this methodology to other Carpathian regions and beyond could provide a unified tool for continuous forest condition assessment, supporting biodiversity conservation, sustainable forest management, and climate resilience strategies. In conclusion, the combination of satellite remote sensing, AI-based segmentation, and Web GIS integration represents a powerful, adaptable solution for modern forest monitoring in mountainous regions, delivering actionable insights for both scientific and practical decision-making.

Acknowledgments

This research was conducted as part of the project “Mapping of the Forest in the National Nature Park Skole Beskids Using Remote Sensing Satellite Data Processing Methods”, which received funding through the EURIZON project, supported by the European Union under grant agreement No. 871072. Also, the authors sincerely thank Dr. Leonid Shumilo (University of Maryland, USA) for his assistance and valuable consultations regarding the improvement and practical implementation of the neural network used in this work.

Declaration on Generative AI

During the preparation of this work, the authors used DeepL for grammar and spelling checks. All content generated or suggested by this tool was carefully reviewed, edited, and approved by the authors, who take full responsibility for the final content of the publication.

References

[1] Y. Averyanova, M. Zaliskyi, O. Solomentsev, O. Holubnychyi, I. Ostroumov, O. Sushchenko, Y. Bezkorovainyi, K. Cherednichenko, O. Sokolova, V. Ivannikova, R. Voliansky, B. Kuznetsov, I. Bovdui, T. Nikitina, Algorithm of wind-related hazards prediction for UAS flight and urban operations based on meteorological data fusion, in: M. Zaliskyi, N. Rizun, I. Ostroumov, L. Tereshchenko (Eds.), Proceedings of the International Workshop on Algorithms of Data Processing (ADP 2024), Kyiv, Ukraine, November 5, 2024, volume 3895 of *CEUR Workshop Proceedings*, CEUR-WS.org, 2024, pp. 132–142. URL: https://ceur-ws.org/Vol-3895/paper11.pdf.

[2] M. Mngadi, I. Germishuizen, O. Mutanga, R. Naicker, W. Maes, O. Odebiri, M. Schroder, A systematic review of the application of remote sensing technologies in mapping forest insect pests

and diseases at a tree-level, Remote Sensing Applications-Society and Environment 36 (2024) 101341. doi:10.1016/j.rsase.2024.101341.

[3] B. Kuznetsov, I. Bovdui, T. Nikitina, R. Voliansky, O. Sushchenko, Y. Bezkorovainyi, Y. Averyanova, I. Ostroumov, O. Solomentsev, O. Holubnychyi, M. Zaliskyi, K. Cherednichenko, O. Sokolova, V. Ivannikova, Efficiency of overhead power lines magnetic field combined electromagnetic silence, in: M. Aghaei, X. Zhang, H. Ren (Eds.), Fifth International Conference on Green Energy, Environment, and Sustainable Development (GEESD 2024), volume 13279, International Society for Optics and Photonics, SPIE, 2024, p. 1327907. doi:10.1117/12.3043769.

[4] A. Candotti, M. De Giglio, M. Dubbini, E. Tomelleri, A Sentinel-2 Based Multi-Temporal Monitoring Framework for Wind and Bark Beetle Detection and Damage Mapping, Remote Sensing 14 (2022) 6105. doi:10.3390/rs14236105.

[5] T. Kuemmerle, O. Chaskovskyy, J. Knorn, V. C. Radeloff, I. Kruhlov, W. S. Keeton, P. Hostert, Forest cover change and illegal logging in the Ukrainian Carpathians in the transition period from 1988 to 2007, Remote Sensing of Environment 113 (2009) 1194–1207. doi:10.1016/j.rse.2009.02.006.

[6] Y. Sokolovskyy, O. Sinkevych, R. Voliansky, Development the Software for Simulation of Physical Fields in Wood Drying Chambers by Using Cellular Automata, in: 2019 IEEE 15th International Conference on the Experience of Designing and Application of CAD Systems (CADSM), 2019, pp. 1–4. doi:10.1109/CADSM.2019.8779262.

[7] F. B. D. S. Mota, K. R. Ferreira, M. I. S. Escada, Evaluating Forest Disturbance Detection Methods based on Satellite Image Time Series for Amazon Deforestation Alerts, The International Archives of the Photogrammetry, Remote Sensing and Spatial Information Sciences XLVIII-3-2024 (2024) 357–364. doi:10.5194/isprs-archives-XLVIII-3-2024-357-2024.

[8] O. Sushchenko, Y. Bezkorovainyi, O. Solomentsev, M. Zaliskyi, O. Holubnychyi, I. Ostroumov, Y. Averyanova, V. Ivannikova, B. Kuznetsov, I. Bovdui, T. Nikitina, R. Voliansky, K. Cherednichenko, O. Sokolova, Algorithm of Determining Errors of Gimballed Inertial Navigation System, in: O. Gervasi, B. Murgante, C. Garau, D. Taniar, A. M. A. C. Rocha, M. N. Faginas Lago (Eds.), Computational Science and Its Applications – ICCSA 2024 Workshops, volume 14816 of *Lecture Notes in Computer Science*, Springer Nature Switzerland, Cham, 2024, pp. 206–218. doi:10.1007/978-3-031-65223-3_14.

[9] K. Cherednichenko, V. Ivannikova, O. Sokolova, I. Ostroumov, O. Sushchenko, Y. Averyanova, M. Zaliskyi, O. Solomentsev, Y. Bezkorovainyi, O. Holubnychyi, B. Kuznetsov, I. Bovdui, T. Nikitina, R. Voliansky, Simulation modelling for urban transport infrastructure optimization in ukraine, in: O. Prentkovskis, I. Yatskiv (Jackiva), P. Skačkauskas, M. Karpenko, M. Stosiak (Eds.), TRANSBALTICA XV: Transportation Science and Technology, Lecture Notes in Intelligent Transportation Infrastructure (LNITI), Springer Nature Switzerland, Cham, 2025, pp. 367–380. doi:10.1007/978-3-031-85390-6_35.

[10] K. Cherednichenko, V. Ivannikova, O. Sokolova, I. Ostroumov, O. Sushchenko, Y. Averyanova, M. Zaliskyi, O. Solomentsev, Y. Bezkorovainyi, O. Holubnychyi, B. Kuznetsov, I. Bovdui, T. Nikitina, R. Voliansky, Modelling and optimization of airport security screening system with anylogic simulation: A case of dublin airport, in: O. Prentkovskis, I. Yatskiv (Jackiva), P. Skačkauskas, M. Karpenko, M. Stosiak (Eds.), TRANSBALTICA XV: Transportation Science and Technology, Lecture Notes in Intelligent Transportation Infrastructure (LNITI), Springer Nature Switzerland, Cham, 2025, pp. 381–397. doi:10.1007/978-3-031-85390-6_36.

[11] A. Qadir, S. Skakun, J. Eun, M. Prashnani, L. Shumilo, Sentinel-1 time series data for sunflower (Helianthus annuus) phenology monitoring, Remote Sensing of Environment 295 (2023) 113689. doi:10.1016/j.rse.2023.113689.

[12] B. Kuznetsov, T. Nikitina, I. Bovdui, R. Voliansky, O. Sushchenko, Y. Averyanova, O. Solomentsev, O. Holubnychyi, M. Zaliskyi, Y. Bezkorovainyi, K. Cherednichenko, O. Sokolova, V. Ivannikova, I. Ostroumov, Multi-Objective Design of Nonlinear Robust Tracking Systems Based on Particles Swarm Optimization Algorithms, in: S. Shukla, H. Sayama, K. Tiwari, J. V. Kureethara (Eds.), Data Science and Security, volume 1354 of *Lecture Notes in Networks and Systems*, Springer Nature Singapore, Singapore, 2025, pp. 157–165. doi:10.1007/978-981-96-4880-1_13.

[13] B. Kuznetsov, I. Bovdui, T. Nikitina, R. Voliansky, O. Sushchenko, Y. Averyanova, O. Solomentsev, O. Holubnychyi, M. Zaliskyi, Y. Bezkorovainyi, K. Cherednichenko, O. Sokolova, V. Ivannikova, I. Ostroumov, Microsatellite Magnetic Cleanliness Based on Geometric Inverse Magneto Static Problem Solution, in: S. Shukla, H. Sayama, K. Tiwari, J. V. Kureethara (Eds.), Data Science and Security, volume 1355 of *Lecture Notes in Networks and Systems*, Springer Nature Singapore, Singapore, 2025, pp. 1–8. doi:10.1007/978-981-96-4883-2_1.

[14] J. Stefanski, O. Chaskovskyy, B. Waske, Mapping and monitoring of land use changes in post-Soviet western Ukraine using remote sensing data, Applied Geography 55 (2014) 155–164. doi:10.1016/j.apgeog.2014.08.003.

[15] I. Ostroumov, Y. Bezkorovainyi, O. Holubnychyi, O. Sushchenko, O. Solomentsev, M. Zaliskyi, Y. Averyanova, K. Cherednichenko, O. Sokolova, V. Ivannikova, B. Kuznetsov, I. Bovdui, T. Nikitina, R. Voliansky, Classification of Flight Situation Based on Risk of Flight Level Loss for Improved Airspace Safety, in: I. Ostroumov, K. Marais, M. Zaliskyi (Eds.), Advances in Civil Aviation Systems Development, volume 1418 of *Lecture Notes in Networks and Systems*, Springer Nature Switzerland, Cham, 2025, pp. 319–334. doi:10.1007/978-3-031-91992-3_21.

[16] State Forest Resources Agency of Ukraine, General Characteristics of Ukrainian Forests, 2022. URL: https://forest.gov.ua/en/areas-activity/forests-ukraine/general-characteristic-ukrainian-forests.

[17] National Nature Park "Skole Beskids", Flora, 2025. URL: https://skolebeskydy-park.in.ua/doslidzhuyte/pryroda-parku/flora/.

[18] Lviv Regional State Forestry and Hunting Management, National nature park "skole beskids", 2019. URL: https://web.archive.org/web/20190724152417/https://lvivlis.gov.ua/nature_reserve_fund_state?id=40.

[19] S. Havryliuk, V. Lavnyy, H.-P. Kahle, C. Vonderach, Estimation of vegetation indexes NDVI/EVI in the Google Earth Engine, in: Proceedings of the 72nd Scientific Conference of UNFU, Lviv, 2022, pp. 13–19. In Ukrainian.

[20] A. Jarvis, H. I. Reuter, A. Nelson, E. Guevara, Hole-filled SRTM for the globe : version 4 : data grid, 2018. URL: https://srtm.csi.cgiar.org.

[21] M. Buchhorn, M. Lesiv, N.-E. Tsendbazar, M. Herold, L. Bertels, B. Smets, Copernicus Global Land Cover Layers—Collection 2, Remote Sensing 12 (2020) 1044. doi:10.3390/rs12061044.

[22] B. Yailymov, A. Shelestov, H. Yailymova, L. Shumilo, Google Earth Engine Framework for Satellite Data-Driven Wildfire Monitoring in Ukraine, Fire 6 (2023) 411. doi:10.3390/fire6110411.

[23] B. Yailymov, H. Yailymova, A. Shelestov, L. Shumilo, Monitoring of Fires Caused by War in Ukraine Based on Satellite Data, in: 2023 13th International Conference on Dependable Systems, Services and Technologies (DESSERT), 2023, pp. 1–5. doi:10.1109/DESSERT61349.2023.10416520.

[24] O. Sushchenko, Y. Bezkorovainyi, O. Solomentsev, M. Zaliskyi, O. Holubnychyi, I. Ostroumov, Y. Averyanova, V. Ivannikova, B. Kuznetsov, I. Bovdui, T. Nikitina, R. Voliansky, K. Cherednichenko, O. Sokolova, Features of Designing Control Systems of Tested Aviation Moving Platforms, in: O. Gervasi, B. Murgante, C. Garau, Y. Karaca, M. N. Faginas Lago, F. Scorza, A. C. Braga (Eds.), Computational Science and Its Applications – ICCSA 2025 Workshops, volume 15888 of *Lecture Notes in Computer Science*, Springer Nature Switzerland, Cham, 2026, pp. 140–151. doi:10.1007/978-3-031-97596-7_9.

[25] L. Breiman, Random Forests, Machine Learning 45 (2001) 5–32. doi:10.1023/A:1010933404324.

[26] J. C.-W. Chan, D. Paelinckx, Evaluation of Random Forest and Adaboost tree-based ensemble classification and spectral band selection for ecotope mapping using airborne hyperspectral imagery, Remote Sensing of Environment 112 (2008) 2999–3011. doi:10.1016/j.rse.2008.02.011.

[27] P. O. Gislason, J. A. Benediktsson, J. R. Sveinsson, Random forests for land cover classification, Pattern Recognition Letters 27 (2006) 294–300. doi:10.1016/j.patrec.2005.08.011, Pattern Recognition in Remote Sensing (PRRS 2004).

[28] O. Tokar, O. Vovk, L. Kolyasa, S. Havryliuk, M. Korol, Using the Random Forest Classification for Land Cover Interpretation of Landsat Images in the Prykarpattya Region of Ukraine, in: 2018 IEEE 13th International Scientific and Technical Conference on Computer Sciences and Information

Technologies (CSIT), volume 1, 2018, pp. 241–244. doi:10.1109/STC-CSIT.2018.8526646.

[29] O. Tokar, S. Havryliuk, M. Korol, O. Vovk, L. Kolyasa, Using Multitemporal and Multisensoral Images for Land Cover Interpretation with Random Forest Algorithm in the Prykarpattya Region of Ukraine, in: N. Shakhovska, M. O. Medykovskyy (Eds.), Advances in Intelligent Systems and Computing III, volume 871 of *Advances in Intelligent Systems and Computing*, Springer International Publishing, Cham, 2019, pp. 48–64. doi:10.1007/978-3-030-01069-0_5.

[30] J.-L. Solorio-Ramírez, R. Jiménez-Cruz, Y. Villuendas-Rey, C. Yáñez-Márquez, Random forest Algorithm for the Classification of Spectral Data of Astronomical Objects, Algorithms 16 (2023) 293. doi:10.3390/a16060293.

[31] Z. Sun, G. Wang, P. Li, H. Wang, M. Zhang, X. Liang, An improved random forest based on the classification accuracy and correlation measurement of decision trees, Expert Systems with Applications 237 (2024) 121549. doi:10.1016/j.eswa.2023.121549.

[32] M. Lavreniuk, L. Shumilo, B. Yailymov, N. Kussul, Reviewing Deep Learning Methods in the Applied Problems of Economic Monitoring Based on Geospatial Data, Cybernetics and Systems Analysis 58 (2022) 1008–1020. URL: https://doi.org/10.1007/s10559-023-00535-9. doi:10.1007/s10559-023-00535-9.

[33] C. Senf, D. Pflugmacher, P. Hostert, R. Seidl, Using Landsat time series for characterizing forest disturbance dynamics in the coupled human and natural systems of Central Europe, ISPRS Journal of Photogrammetry and Remote Sensing 130 (2017) 453–463. doi:10.1016/j.isprsjprs.2017.07.004.

[34] B. Hosseiny, M. Zaboli, S. Homayouni, Forest Change Mapping using Multi-Source Satellite SAR, Optical, and LiDAR Remote Sensing Data, ISPRS Annals of the Photogrammetry, Remote Sensing and Spatial Information Sciences X-4-2024 (2024) 163–168. doi:10.5194/isprs-annals-X-4-2024-163-2024.

[35] P. Olofsson, G. M. Foody, M. Herold, S. V. Stehman, C. E. Woodcock, M. A. Wulder, Good practices for estimating area and assessing accuracy of land change, Remote Sensing of Environment 148 (2014) 42–57. doi:10.1016/j.rse.2014.02.015.

[36] S. L. Powell, W. B. Cohen, S. P. Healey, R. E. Kennedy, G. G. Moisen, K. B. Pierce, J. L. Ohmann, Quantification of live aboveground forest biomass dynamics with landsat time-series and field inventory data: A comparison of empirical modeling approaches, Remote Sensing of Environment 114 (2010) 1053–1068. doi:10.1016/j.rse.2009.12.018.

[37] O. Chaskovskyy, S. Havryliuk, O. Sinkevych, A. Nechepurenko, O. Pelyukh, M. Rozumovskyi, Leveraging satellite data to support decision-making on forest disturbances in “Skole Beskids” National Nature Park, in: R. Voliansky, O. Solomentsev, K. Slimani, N. Kuzmenko (Eds.), Proceedings of the International Workshop on Computational Methods in Systems Engineering (CMSE 2025), Kyiv, Ukraine, June 12, 2025, volume 3981 of *CEUR Workshop Proceedings*, CEUR-WS.org, 2025, pp. 182–191. URL: https://ceur-ws.org/Vol-3981/paper16.pdf.